

Canonical Sound Speed Profile and Related Ray Acoustic Parameters in the Bay of Bengal

T.V.RAMANA MURTHY, Y.SADHURAM, M.M.MALLESWARA RAO, B.P.RAO,
S. SURYA PRAKASH, P. CHANDRAMOULI, K.S.R.MURTHY and K.V.S.R.PRASAD¹

National Institute of Oceanography, Regional center, Visakhapatnam - 530 017

¹Department of Meteorology and Oceanography, Andhra University, Visakhapatnam - 530 003

Following Munk's canonical theory, canonical parameters (i.e., B the stratification scale and ε the perturbation coefficient) in adiabatic ocean are obtained using SOFAR channel parameters (i.e., C , sound velocity at the channel axis, Z , the depth of the channel axis) from the CTD data collected on board ORV Sagarkanya Cruise No.30 at 17° 36.21'N, 84° 35.31'E, during March, 11-20, 1987 in the Bay of Bengal to develop the stratified model for implementation in the numerical ray tracing to study the ocean acoustic parameters namely eigen rays, travel time, turning depths, transmission loss etc., for source-receiver configuration kept at channel axis.

The simulated acoustic ray parameters of canonical ocean reveals that the even very flat angle rays can scan entire water column with repeated reflections from both surface and bottom due to depth limited nature of sound channel and weak gradients of sound velocity prevailing in the medium on either side of the sound channel axis. This nature of phenomenon usually occurs in the case of 'shallow-water channel'. This paper also describes degeneracy of the ray paths, which arrive simultaneously. Since the results are generated through simplest sound channel (exponential stratified model) above and beneath the sound axis which are more useful as a priori knowledge before conducting actual sound transmission experiment in the area of interest.

Introduction

Acoustic waves, which travel long distances in the ocean in the form of ducted propagation with less attenuation, relative to other forms of energy, are used in a large number of applications in the ocean (Urlick, 1983). For example, submarine signaling and detection, precise bathymetric measurements, sub-bottom profiling, fish finding etc. This is possible with the tracing of ray paths of sound pulses from a given source to a receiver in the ducted ocean of area of interest. Some of the common forms of ducts are: mixed layer sound channel, deep sound channel and shallow water sound channel. The surface sound channel (i.e., mixed layer sound channel) occurs when the upper layer exhibits isothermally leading to depth wise increase in the sound velocity, due to hydrostatic pressure. In this case the axis of the channel lies close to the sea surface. If an acoustic source is placed within this layer of constant velocity gradient, the acoustic energy gets trapped within this channel and propagation takes place along the rays that are in the form of arc of circles of radius of curvature $R = C_0/g$ where C_0 is surface sound velocity and g is velocity gradient. In the case of deep sound channel transmission experiments, sound sources and receivers are both placed preferably around the SOFAR (Sound Fixing And Ranging) channel axis (i.e., around the locus of points of minimum sound velocity). For example, in the tropical seas the sound velocity is varies from 1 to 1.5 km below the ocean surface. This is

due to the opposing effects of temperature, which dominates in the upper layers and causes a rapid decrease in sound velocity with depth, while the pressure, which increases eventually results in an increase of sound velocity. This configuration of the sound velocity profile in the vertical section of an ocean, which traps the sound rays around the sound axis, is called sound channel or SOFAR channel. Sound rays propagating along the SOFAR channel axis are refracted downward when propagating in the region of negative sound velocity gradient above the level of minimum sound velocity and upward when propagating in the region of positive gradient below it. The important feature of sound propagation along the SOFAR channel is that energy losses due to geometric spreading and scattering associated with the boundaries are minimized and consequently large ranges of sound propagation are possible for the same source power (Officer, 1958). Since the sound velocity increases above and below the sound channel axis due to temperature and pressure, the profile can be mathematically expressed as linear combination of exponential and linear functions. Munk (1974) derived an expression for sound channel in an exponentially stratified ocean with application in SOFAR channel and named as Canonical Sound Channel (CSC) This profile is directly from thermodynamic constants, a temperature and salinity linear $\theta - s$ relation, and the assumption of an exponential profile in buoyancy frequency $n = n_0 e^{2/B}$ wherein n_0 is buoyancy surface extrapolated value and B is ocean stratification relation. Ramana Murty, *et.al* (1989) developed an algorithm for obtaining CSC parameters from CTD data and applied to Bay of Bengal. This CSC profile enables us to present the sound-velocity profile at any geographical location with the help of a few parameters obtained from hydrographic data, apart from its implication in ray tracing and normal mode theory (Williams, 1970). Numerical simulation of acoustic parameters is very important aspect using simplest CSC profile from historical/insitu data for any transmission experiment for determining stable eigen rays (rays connecting between source to receiver) and anticipated degeneracy rays. Numerical experiments using acoustic models in analytical (canonical) ocean without introducing complexity in the system, are essential for the success of any transmission experiment as a priori knowledge.

In the present study, some numerical experiments are done to find out eigen rays and related ray parameters following the example of Munk's canonical sound velocity profile for continental slope waters off Visakhapatnam during March 11-20, 1987. These results are useful for acoustic field measurements.

Mathematical Formulation

The hypothetical source $S(x_0, z_0)$ and receivers (s) R_i (Where, $i = 1, 2, \dots, n$) located along a vertical section of the transmitting medium (Fig.1) are separated by several kilometers. Following Aurthur *et al*, 1952, the ray geometry is governed

by
$$\frac{dx}{ds} = \cos \theta \dots \dots \dots (1)$$

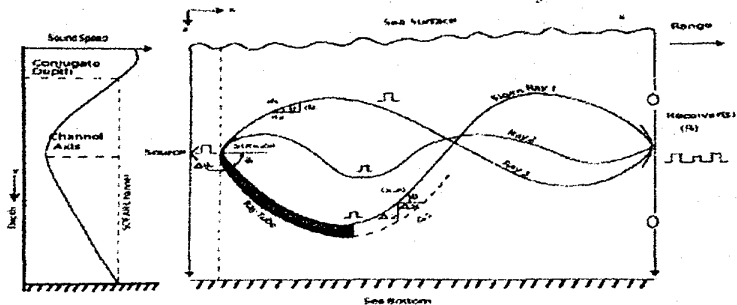


Fig.1: Schematic presentation of acoustic rays from source to receiver

$$\frac{dz}{ds} = \sin \theta \quad \dots \dots \dots (2)$$

$$\frac{d\theta}{ds} = \frac{1}{C} \left[\sin \theta \frac{\partial C}{\partial x} - \cos \theta \frac{\partial C}{\partial z} \right] \quad \dots \dots \dots (3)$$

where, θ is the angle of emergence of sound ray (Fig.1) and s is the arc length along the ray. The eqs. (1) - (3) describe the ray paths and the numerical integration of these equations for a given sound velocity distribution, provides the coordinates of the Eigen ray paths (Ramana Murty and Mahadevan, 1994). Once the eigen rays are identified from the ray computation, the time of flight (T_i) and ray intensity (using ray tube method) are calculated from following equations.

$$T_i = T_s + \sum_{j=1}^4 \{ (x_j - B_j Z_j) + (y_j - B_j Z_j) \} A_j ds \quad \dots \dots \dots (4)$$

where, i covers full range.

Intensity computations—The acoustic intensity at any point along the ray path is given by the expression (Krol, 1979).

$$Intensity = I(x) / I_0 = (\sin \theta_0 / x \cos \theta) (\Delta \theta_0 / \Delta z) \quad \dots \dots \dots (5)$$

where, I_0 = reference intensity at the source; θ_0 = eigen ray angle at the source with reference to the horizontal; θ = ray angle at the point of measurement with reference to the horizontal; x = distance from the source to the point of measurement; Δz = vertical distance at the point of measurement between eigen ray and ray in its immediate vicinity, $\Delta \theta_0$ = angle between eigen ray and ray in its immediate vicinity at the source.

At the point where $\Delta z \rightarrow 0$ the above expression will not hold good (tends to infinity mathematically) and the previous value only gets substituted for computational continuity. Considering the phase shift for any given frequency the intensity has been computed following the method by Moler & Soloman (1970).

$$\begin{aligned} I/I_0 &= \left| \sum P_i e^{i2\pi f t_i} \right| \\ &= \sum_j \sum_k P_j P_k \cos[2\pi f(t_j - t_k)] \end{aligned} \quad \dots \dots \dots (6)$$

where, $P_k = [I_k(x)/I_0]^{1/2}$ and t_k are the relative pressures and arrival times of the eigen rays. These have wider applications in signal detection.

Computation of canonical sound speed profile

For simulation studies a parametric representation of the sound-velocity profile is needed. In the present study, we construct a representative sound velocity profile of waters of Visakhapatnam in an analytical form following Munk (1974). The mathematical expression for generation of canonical sound velocity profile has been detailed. The theory enables us to present the sound-velocity profile at any geographical location with the help of a few parameters obtained from hydrographic data, apart from its implication in ray theory and normal mode theory. The Canonical expression for the sound velocity profile $C(Z)$ (Munk, 1974) expressed as function of a depth, stratification scale and perturbation coefficient as follows:

$$C(Z) = C_1 [1 + \varepsilon(ZW/B) + \exp(-2W/B) - 1] \quad \dots \dots \dots (7)$$

where $W = Z - Z_1$, (Z_1 is depth of sound channel axis)

$B = a/b$ (Stratification scale), $\varepsilon = a^3/b^2$ (Perturbation coefficient)

$$a = \sqrt{\frac{r_1 \mu_3 - r_2 \mu_2}{\mu_1 \mu_3 - \mu_2^2}}, \quad b = \sqrt[3]{\frac{r_1 \mu_2 - r_2 \mu_1}{\mu_1 \mu_3 - \mu_2^2}}$$

$$\mu_1 = \int_{-a}^{\beta} W^4 dW, \quad \mu_2 = \int_{-a}^{\beta} W^3 dW, \quad \mu_3 = \int_{-a}^{\beta} W^6 dW, \quad \dots \dots \dots 8 \text{ (a,b,c)}$$

$$r_1 = \int_{-a}^{\beta} [f(W) - 1] W^2 dW \quad \dots \dots \dots 8 \text{ (d)}$$

$$r_2 = \int_{-a}^{\beta} [f(W) - 1] W^6 dW \quad \dots \dots \dots 8 \text{ (e)}$$

The above integrals can be evaluated using natural cubic spline interpolation technique for given sound velocity profile, depth of sound channel axis, velocity of sound at channel axis and upper and lower limits of sound velocity profile to get stratification scale and perturbation coefficient.

Results and Discussions

Generation of canonical sound speed profile

Data on temperature, salinity in the shelf waters off Visakhapatnam collected during March, 11-20, 1987 on ORV Sagarkanya (Cruise No.30 at 17° 36.21'N, 84° 35.31'E) has been used to generate canonical sound velocity profile

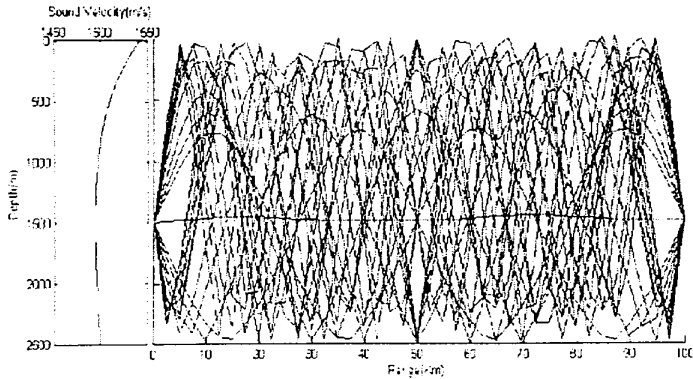


Fig.2: Eigenrays for a source depth of 1490m and receiver depth of 1490m over 100km range in canonical ocean off Visakhapatnam

based on the algorithm developed by Ramana Murty *et.al*, (1989) (as input profile) for conducting numerical acoustic modeling. The data was subjected to cubic spline (for continuous data) and weighted parabolic (for discrete data) interpolation (Reininger and Ros, 1968) to obtain observations at closely spaced depth intervals (10m). Using the data sound velocity has been computed following Chen and Millerio (1977) to obtain the sound velocity at the channel axis (C_1), the depth of the channel axis (Z_1) and upper and lower bounds of integration ($-\alpha, \beta$) for the integrals appearing in Eqs.8 (a-e) for computation of the stratification scale B and perturbation coefficient ϵ . Here α is the conjugate depth (depth below the sea surface at which the sound velocity equals the near bottom value at the depth β).

Computed Canonical sound channel model parameters are

$$\alpha = 250 (m), \beta = 2490 (m), Z_1 = 1490 (m), C_1 = 1493.72 (m/s)$$

$$B = 1.4148339 (km), \epsilon = 6.27009 \times 10^{-3}$$

Using above Canonical sound channel model parameters, the Munk's canonical sound velocity profile is generated using Eq. 7. The generated profile using Eq. (7) describes the simplest sound channel that has built-in the fundamental asymmetry between the ocean above and beneath the sound axis shown in Fig.2 (left panel). It will serve as analytical guide to the subsequent discussion on path resolution and identification and also utilized for the numerical ray tracing to study the ocean acoustic parameters.

Eigen rays: Acoustic rays were traced using a range - independent software (RamanaMurty*et.al*,2005) for emergence angles between $+12^\circ$ and -12° at 0.1 intervals. The canonical profile (Fig 2, left panel) is used for the ray tracing. A source depth of 1490 m corresponding to the depth of the SOFAR channel axis, and a receiver depth of again was 1490 m over a range of 100 km were selected for computing the eigen rays shown in Fig.2 (rightpanel).The ray parameters at source and receiver obtained from these computations are presented in Table1.

S no	θ_0 (deg)	θ_r (deg)	Σds (m)	p^+	p^-	p_t^+	p_t^-	$p_t^+ + p_t^-$	$F_t^+ + F_t^-$	T (s)	I/I_0 (10 ⁻¹)	- dB
1	-0.32853	0.32854	104960	6	7	6	7	13	13	69.852	7.8050	50.538
2	-0.31305	-0.31305	104400	6	6	6	6	12	12	69.436	7.4240	50.644
3	-0.28613	0.28613	103600	5	6	5	6	11	11	68.909	7.0870	50.748
4	-0.27424	-0.27425	103120	5	5	5	5	10	10	68.544	6.6550	50.884
5	-0.25368	0.25368	102500	4	5	4	5	9	9	68.102	4.1620	51.903
6	-0.24688	-0.24688	102170	4	4	0	4	8	4	67.779	0.1519	59.092
7	-0.18822	0.18821	101270	3	4	0	4	7	4	67.458	0.1458	59.181
8	-0.15733	-0.15731	100830	3	3	0	3	6	3	67.241	0.1495	59.127
9	-0.12036	0.12036	100460	2	3	0	3	5	3	67.096	0.1086	59.821
10	-0.09775	-0.09775	100250	2	2	0	2	4	2	66.975	6.6130	50.898
11	0.002099	2.86E-06	99977	2	2	0	0	4	0	66.931	0.3329	57.388
12	0.057754	0.097754	100256	2	2	0	2	4	2	66.975	6.6080	50.900
13	0.12395	-0.12396	100470	3	2	0	2	5	2	67.069	0.1554	59.043
14	0.15733	0.15733	100430	3	3	0	3	6	3	67.241	0.1497	59.124
15	0.21345	-0.21345	101550	4	3	0	3	7	3	67.483	0.1542	59.060
16	0.24703	0.24703	102170	4	4	0	4	8	4	67.781	0.1609	58.967
17	0.26214	-0.26214	102690	5	4	5	4	9	9	68.198	5.3300	51.366
18	0.27425	0.27424	103120	5	5	5	5	10	10	68.544	6.6710	50.879
19	0.29612	-0.29612	103860	6	5	6	5	11	11	69.04	7.4160	50.649
20	0.31305	0.31305	104400	6	6	6	6	12	12	69.436	7.4770	50.631
21	0.33821	-0.33821	105260	7	6	7	6	13	13	70.017	8.2280	50.424

Table 1- θ_0 - ray launching angle at source, θ_r - ray angle at receiver, ds - ray path length, p^+ - number of upper turning points, p^- - number of lower turning points, p_t^+ - number of top bonks, p_t^- - number of bottom bonks, T - travel time, I/I_0 - acoustic intensity ratio, dB - decibel (unit of intensity).

The columns 5 to 10 of Table 1 explain number of upper (p^+) and lower (p^-) ray turnings, number of top (p_t^+) and (p_t^-) bottom ray bonks, and total number of ray turnings and bonks respectively. This information can be used as ray identifier. The ray identifier enables us to identify the rays from their arrival patterns, since the rays usually arrive at the receiver in groups. There are four classes of rays 1) R/R (purely refracted both above and beneath the axis, ($p_t^+ = p_t^- = 0$)) 2) SR/R (surface reflected and refracted, $p_t^+ \neq 0$, $p_t^- = 0$), 3) R/BR (refracted and bottom reflected, $p_t^+ = 0$, $p_t^- \neq 0$) 4) SR/BR (surface and bottom reflected, $p_t^+ \neq 0$, $p_t^- \neq 0$). In case of northern Indian Ocean, the effective wave-guide is below the 100m depth. Keeping the source and receiver in these SOFAR channels, rays may not propagate in the upper layers above 100 m depth (Prasanna kumar, *et.al*, 1994). But in tropical regions, the monsoon eddies generated by winds etc., cannot be monitored effectively by keeping the acoustic source and receivers in SOFAR systems. But the present results reveal that in the coastal waters of Visakhapatnam, even flat angle rays are covering the top layer indicating the possibility of monitoring the monsoon eddies due to external and internal forcing mechanisms. Numerical experiments of off-shore waters of Visakhapatnam (Fig 2 and Table 1) depict that there are 21 eigen rays comprising three classes rays with 10, SR/BR , 10 R/BR and one R/R . SR/R ray class is missing among the 4 classes which may be due to depth-limited nature of the sound velocity profile. These 3 classes of rays are scanning the entire shelf water column with repeated surface and bottom reflections with very small marginal grazing eigen angles with -0.32853° to 0.33821°

(column 2 of Table 1), which is very much lesser than the flat and limiting angles of sub-surface duct of deep water structure (Prasanna kumar, *et.al*,1994) exhibited as the case of propagation takes place in the 'shallow water channel'.

Travel time: Fig 3 depicts flight of travel times (T) of sound pulses from source to receiver (using Eq.4) versus intensity losses (spreading losses) at the receiver (Eq.5) in graphical form where as the numerical values are presented in Table 1 (columns 11 and 12). For *normal* sound channel, *steep* rays with turning points near the surface and bottom (where the sound velocity is large) are the first refracted rays to arrive, even though their path length is the longest, flat (or axial) rays come in last. In the present case, arrival of steep angle rays comes last than the flat angles, which is contradicting the arrival pattern of normal sound channel of other waters. From the Fig.3 and Table 1 (column 11), the span (first arrival to last arrival) of arrival pattern of the rays is within small marginal of 3.086 seconds, attributed to the weak acoustic wave-guide nature of the tropical shelf waters off Visakhapatnam. From the rays arrival structure shown in Fig.2 and Table 1 it is seen that the near axial $\pm R/BR$ rays present poor resolution (< 0.81 sec) though they are the first arrivals while SR/BR rays have a relatively better resolution (< 1.9 sec) and they are last arrivals. This temporal resolution is sufficient to distinguish multi path arrivals estimated with in the range of 50 m for monitoring the mesoscale eddies etc. Another interesting feature of these waters is R/R ray, so called *channel axis ray* having no upper and lower turnings not covering water column (Fig.2) happen to be the first arrival (Table 1) and this phenomenon is uncommon compared to other waters of the ocean. This channel axis ray always presents, in all the world oceans with less attenuation and it is presumed to be the only one to survive the very long transmission range. The changes in the ocean temperature due to Green house effect can be measured by conducting experiments over a decade, keeping the powerful sources at the channel axis (Munk and Forbes, 1989). This axial arrival pattern is useful information for matching and identification of the acoustic signal measurements with predicted arrival pattern based on the theory at the receiver end and to enable to get anomaly of the travel times. These arrival anomalies are operated with Generalized Inverse Operator (GIO) to get perturbations of temperature field due to thermocline displacements caused by eddies, meanders, currents, barocline instability of water column etc.(Ramana Murty, *et.al*,1996).

Acoustic Intensity: The attenuation of sound intensity along a ray path in a propagating medium is due to geometric spreading, absorption losses and scattering at the boundaries. In case of sound propagation in SOFAR channel the wave rays, which refract internally do not encounter boundaries and the attenuation is mainly due to cylindrical spreading and losses due to boundary scattering is completely absent. The transmission loss at any point in a SOFAR channel due to geometrical spreading can be estimated in terms of the vertical spacing between

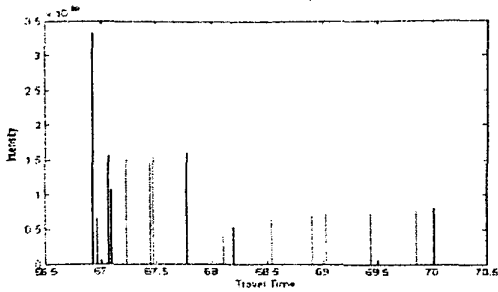


Fig.3: Travel times versus intensity losses

rays (ray tube) that are adjacent at the source and pass around the point of interest (Fig.1). The computed cylindrical spreading (physical losses) using ray tube method (Eq.5) at receiver end are shown in Fig.3 and the corresponding numerical values are presented in Table 1. The intensity losses of the 21 eigen rays at the receiver showed variation from about 51.42 dB to 59.81dB. The loss associated with steep angle rays is less compared to the flat angle rays because the steep angle rays sample the upper layer of the ocean (having relatively strong sound velocity gradients) more often than other rays. In the present simulation experiment, intensity loss also has been computed considering the phase shift (Table 1, column 10) with short-range frequency of 400 Hz using Eq.6. The computed cumulative intensity losses for all the 21 eigen rays, 10 *SR/BR* and 10 *R/BR* are found to be -95.47 dB, -91.78 dB, -98.61 dB respectively. Here *R/BR* rays suffer more as compare to *SR/BR* this may be due to propagation take place less refractive media. These simulated ray arrival times and their energy level provide a basis for the identification on the measured ray arrival structure during acoustic field experiments. In addition to the above information, the following analysis of ray degeneracy of waters in the area of interest based on the historical or insitu data has been done for identification and resolution of ray paths which is a very important aspect for acoustic signal processing during actual field experiments.

Ray degeneracy: Ray arrival structure is complicated. Rays come in groups: group p , for example, contains $+p, p; -p, p; +p+1, p; -p, p+1$; to be followed by group $p+1, +p, p$. The arrival sequence and spacing of the four constituents within a group depends on the depths of source and receiver, and the group number itself. Two constituents can arrive simultaneously, and this degeneracy causes trouble with resolution and identification. There are three circumstances where two ray paths can arrive simultaneously: (1) Up-down degeneracy (2) channel asymmetry degeneracy (3) turning point degeneracies. The definition of these are given in Munk and Wunsch (1979). Degeneracy of ray paths can be analyzed based information on eigen angles, number of upper ($+p$) and lower ray turnings ($-p$), ray path lengths and arrival times which are given in the Table-1. The following analysis has been made for the shelf waters of Visakhapatnam for obtaining the identification of degeneracy.

(1). Up-down degeneracy $\pm p$, p : (\pm) 0.31305° , 0.2742° belong to *SR/BR* ray type belongs to up-down degeneracy rays, since they have the same source and receiver depth and number of turning depths are equal.

(2) Channel asymmetry degeneracy $+p+1$, p with $-p$, $p+1$. The Eigen angle 0.28813° of ray type having up-down turning points (5,6) with Eigen angle 0.29812° of same ray type having up-down turning points (6,5) reaching receiver late by 0.131seconds come under channel asymmetry degeneracy

(3) Turning point degeneracies: The Eigen angles 0.25366° of *SR/BR* type having number of turning points (4,5) with an angle -0.26214° of same type reaching receiver late by 0.09 seconds comes under Turning point degeneracy.

Conclusions

Following Munk's Canonical theory, analysis on acoustic propagation characteristics in the coastal waters off Visakhapatnam (during March, 11-20, 1987) using ray model has been discussed. Model results reveal that there are three classes of eigen rays consisting of *R/R*, *SR/BR* and *R/BR* scan the entire water column (with small eigen angles between -0.32853° to 0.33821°), which are of the order of much lesser than the critical angle of sub-surface ducts. This channel is attributed as the weak wave-guide and also concluded as the case of propagation that occurs in *shallow water channel*. The span of simulated travel times of the eigen rays at the receiver end were found to be within small margin of 3.086 seconds having intensity loss variation from 51.42 dB to 59.81 dB indicated that the possibility of monitoring the sea sub-surface mesoscale variability, in addition to deep water eddies. Apart from the above aspects, anticipated ray degeneracy was explained for ray identification and temporal resolution, which are useful for acoustic signal processing of field measurements.

Acknowledgements

The authors are thankful to Dr.S.R.Shetye, Director, National Institute of oceanography, for his constant encouragement and keen interest in this study.

References

1. Arthur,P.S, Munk,W.H, Isaac,J.D., 1952, The direct construction of waves rays, Trans.amer.Geophys.union, 33, pp. 855-865.
2. Chen C T and Millero F J. 1977, Speed of sound in sea water at higher pressure; J.Acoust.Soc,Am.55, 129-135.
3. Krol H R, "Intensity calculations along a single ray", J Acoust Soc Am, 53(1973)864.
4. Moler C.B & Solomom L.P, 1970, Use of splines and numerical integration in geometrical acoustics, J Acoust Soc Am, vol.48 pp 739.
5. Munk W.H, 1974, Sound channel in an exponentially stratified ocean with application to SOFAR; J.Acoust.Soc.Am, vol.55, pp. 220-226.
6. Munk W.H & Wunsch.C, 1979 ,Ocean acoustic tomography:a scheme for large scale monitoring; Deep Sea Res.Am, vol.55 pp 220-226.
7. Munk.W.H & Forbes A.M.G, 1989, "Global ocean warming: An Acoustic Measure", J.Phys Oceanogra, Vol.15, pp.1765-1778.

8. **Officer C.B**, 1958, *Introduction To The Theory Of Sound Transmission*, McGraw-Hill, Inc. USA.
9. **Prasanna Kumar.S, Navelkar.S.G, Ramana Murty.T.V & C.S.Murty**, 1994, Acoustic propagation within a surface duct in the western Bay of Bengal, *Indian Journal of Marine Sciences*, vol.23, pp-236-238.
10. **Prasanna kumar.S, Ramana Murty.T.V, Somayajulu.Y.K, P.V.Chodankar & C.S.Murty**,1994, Reference Sound Speed Profile and Related Ray Acoustics of Bay of Bengal for Tomographic Studies,*Acustica*,vol.80, pp127-137.
11. **Ramana Murty T V, Prasanna Kumar S, Somayajulu Y K, Sastry J S and Rui J P De Figueiredo**, 1989, Canonical sound speed profile for the central Bay of Bengal. *Earth Planet Sci.*, Vol 98, No: 3, pp 255-263.
12. **Ramana Murty.T.V, Mahadevan.R**, 1994, *Stochastic Inverse Method for Ocean Acoustic Tomography Studies - A Simulation Experiment*, IIT Technical Report No.31.
13. **Ramana Murty.T.V, Somayajulu.Y.K & C.S.Murty**, (1996), Reconstruction of sound speed profile through natural generalized inverse technique, *Indian J Mari. Sci*,vol.25,pp.328-334.
14. **Ramana Murty T V, Somayajulu Y K & Sastry J S**, 1990, Computations of some acoustic ray parameters in the Bay of Bengal, *Indian J Mari. Sci*, Vol. 19, pp.235-245.
15. **Ramana Murty.T.V,M.M.Malleswara Rao, S.Surya Prakash, P.Chandramouli & K.S.R.Murthy**, 2005 , *Algorithms and Interfaces for Ocean acoustic ray-tracing*, Report NIO.TR No.09/2005.
16. **Reiniger R F and Ros C K**, 1968, A method of interpolation with application to oceanographic data; *Deep Sea Res.*55, pp.185-193.
17. **Urlick,R.J**, 1983, *Principles of Underwater Sound*, McGraw-Hill, Inc.
18. **Willams.A.O**, 1970, "Normal mode methods in propagation of under water sound In *Underwater Acoustics*, ed.R.W.B.Stephens ,(Wiley-Interscience, New York).